

Electrical Transport and Photovoltaic Behavior of $\text{Cu}_2\text{ZnSnSe}_4$ Heterojunctions: Insight from Dark I–V and Differential Analysis

N.N. Mursakulov*, S.G. Nuriyeva Azizova*, N.N. Abdulzade, Sh.M. Azizov, I.G. Nuriyev

Institute of Physics, Ministry of Science and Education of the Republic of Azerbaijan, G. Javid Ave. 131, AZ1073 Baku, Azerbaijan

Abstract: - The electrical transport and photovoltaic behavior of $\text{Cu}_2\text{ZnSnSe}_4$ (CZTSe)-based heterojunctions were investigated using dark current–voltage (I–V), semi-logarithmic, and differential analysis techniques. The dark I–V characteristics exhibit nonlinear diode-like behavior, indicating the formation of a potential barrier at the heterointerface. Semi-logarithmic and $\ln(I)$ –V analyses reveal a linear region, confirming that carrier transport is primarily governed by thermionic emission mechanisms.

The ideality factor was determined from the $\ln(I)$ –V slope as $n \approx 2.4$, indicating non-ideal diode behavior associated with recombination and interface-related processes. The saturation current and barrier height were estimated as $I_0 \approx 1 \times 10^{-7}$ A and $\Phi_b \approx 0.8$ eV, respectively. At higher forward bias, deviations from ideal behavior were attributed to series resistance effects, with $R_s \approx 60 \Omega$.

Differential conductance and resistance analyses reveal voltage-dependent carrier transport and provide additional sensitivity to interface-controlled conduction processes. Under AM1.5G illumination, the heterojunction exhibits a clear photovoltaic response characterized by photocurrent generation and open-circuit voltage formation.

These results provide insight into non-ideal transport mechanisms and demonstrate the role of interface properties in determining the performance of CZTSe-based heterojunctions for thin-film photovoltaic applications.

Keywords: $\text{Cu}_2\text{ZnSnSe}_4$; heterojunction; electrical transport; dark I–V characteristics; differential analysis; thermionic emission; photovoltaic response

1. INTRODUCTION

$\text{Cu}_2\text{ZnSn}(\text{Se},\text{S})_4$ (CZTSSe) compounds have emerged as promising absorber materials for thin-film photovoltaic applications due to their earth-abundant, low-toxicity constituents and suitable optoelectronic properties [1,2]. In particular, $\text{Cu}_2\text{ZnSnSe}_4$ (CZTSe), representing the selenium-rich end member of the CZTSSe system, exhibits a direct bandgap and a high absorption coefficient, enabling efficient light harvesting even in thin layers. Magnetron sputtering is considered an effective technique for CZTSe thin-film deposition due to its ability to produce uniform and high-quality absorber layers with controlled composition [3,4].

However, despite these advantages, the performance of CZTSSe-based heterojunction devices remains significantly below theoretical limits [5,6]. This limitation is primarily attributed to high recombination losses, interface defects, and non-ideal charge transport mechanisms [7,8]. Structural disorder and the presence of secondary phases introduce defect states that act as recombination centers, thereby degrading carrier collection efficiency [9,10].

Electrical transport analysis plays a key role in understanding these limitations. While conventional current–voltage (I–V) characterization provides basic information about diode behavior, it is often insufficient to resolve complex transport processes dominated by interface-controlled conduction and recombination effects [11,12]. In particular, non-ideal transport behavior in CZTSe heterojunctions requires more sensitive analytical approaches [13,14].

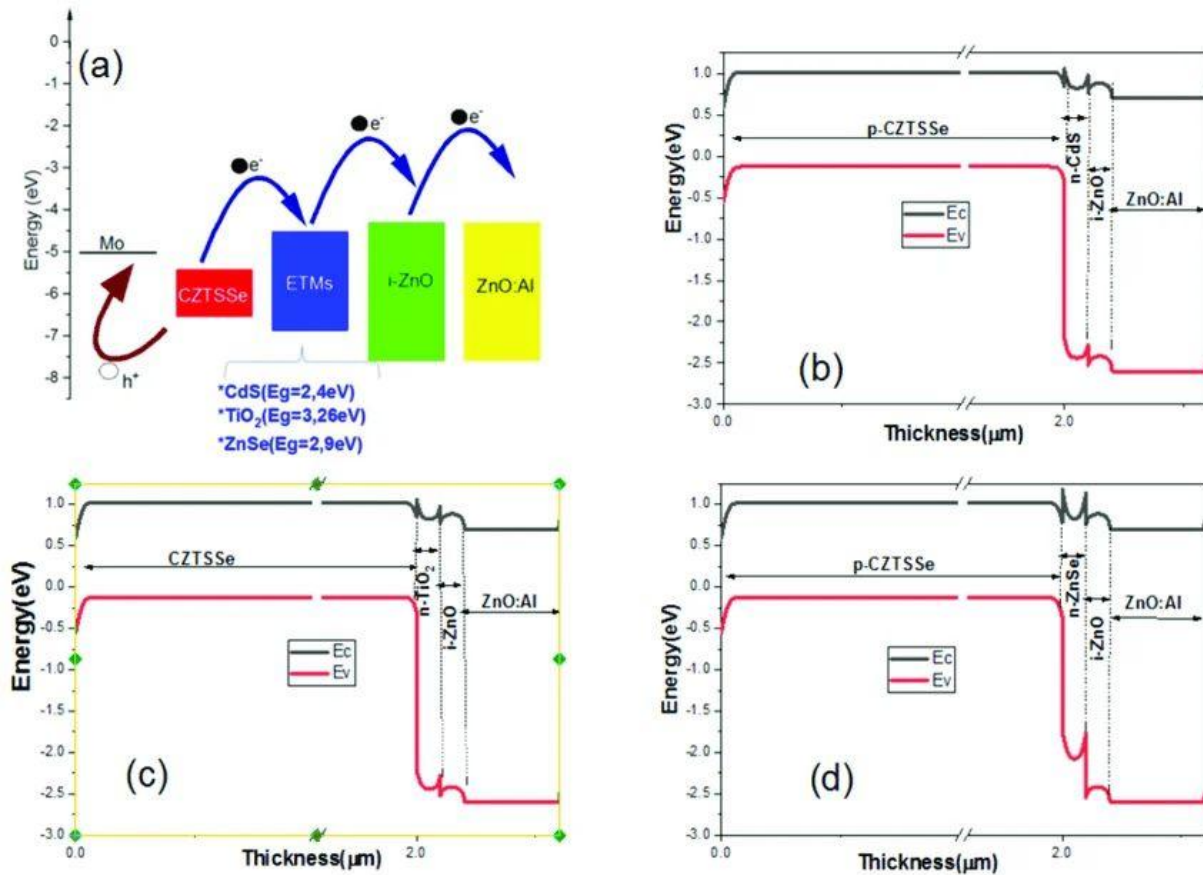


Figure 1. Schematic representation of the CdS/Cu₂ZnSnSe₄ (CZTSe)/Mo heterojunction device architecture along with the corresponding energy band diagram under illumination.

The figure illustrates photogeneration within the CZTSe absorber, band bending at the heterointerface, efficient separation of electron–hole pairs, and directional carrier transport toward the front (CdS) and back (Mo) electrical contacts.

In this context, differential transport analysis, including differential conductance (dI/dV) and differential resistance (dV/dI), provides enhanced sensitivity to voltage-dependent transport mechanisms and enables more precise identification of interface-related conduction processes [15,16]. Despite its importance, such analysis remains insufficiently explored for CZTSe-based heterojunctions [17,18].

In this work, the electrical transport and photovoltaic behavior of CZTSe-based heterojunctions are investigated using a combined approach based on dark I–V characteristics, semi-logarithmic analysis, and differential parameter evaluation. The aim is to identify dominant transport mechanisms, quantify non-ideal diode parameters, and clarify the role of interface-controlled processes in determining device performance [19,20]. Additionally, the photovoltaic response under AM1.5G illumination is analyzed to establish the relationship between electrical transport and photoelectric behavior [5,6].

2. EXPERIMENTAL DETAILS

The electrical transport properties of the Cu₂ZnSnSe₄ heterojunction were investigated using dark current–voltage (I–V) measurements [1,2]. A stabilized DC voltage source (B5-47) was used to apply the bias voltage, while the resulting current was recorded using a high-precision Keithley 2000 digital multimeter, enabling reliable detection of low-current signals under high-sensitivity measurement conditions [3,4].

Photovoltaic characterization was performed under AM1.5G simulated solar illumination using a calibrated solar simulator [5,6]. The illumination intensity was adjusted to standard test conditions (100 mW/cm²) [5]. The measurement setup employed for electrical characterization, including the Keithley 2000 digital multimeter, is shown in Fig. 2.



Figure 2. Keithley 2000 digital multimeter used for electrical measurements of the $\text{Cu}_2\text{ZnSnSe}_4$ heterojunction.

The corresponding current density–voltage (J – V) characteristics were derived from the I – V data to evaluate the photoresponse of the heterojunction [7,8]. In addition, differential conductance (dI/dV) and differential resistance (dV/dI) were numerically calculated from the experimental data for further analysis [9,10]. The AM1.5G illumination system used for photovoltaic measurements is presented in Fig. 3 [6].



Figure 3. AM1.5G simulated solar illumination system employed for photovoltaic characterization.

All measurements were carried out at room temperature ($T \approx 300$ K) and repeated at least three times to ensure reproducibility [11].

3. RESULTS AND DISCUSSION

3.1 Dark I – V and J – V Characteristics

The relatively small thickness of the CZTSe layer (~ 100 nm) may also contribute to enhanced recombination effects due to incomplete light absorption and increased influence of interface states. Similar behavior has been reported in ultrathin kesterite absorbers [5].

The dark current–voltage (I – V) and current density–voltage (J – V) characteristics of the $\text{Cu}_2\text{ZnSnSe}_4$ (CZTSe)-based heterojunction are presented in Figure 4. Both representations exhibit pronounced nonlinear behavior, confirming diode-like electrical transport. Under forward bias, the current and current density increase exponentially with applied voltage, indicating the formation of a potential barrier at the heterointerface. In the reverse bias region, the relatively low current density suggests weak leakage currents and acceptable interface quality [7,8].

The use of J – V representation allows normalization with respect to device area and provides a more accurate description of carrier transport behavior in the heterojunction.

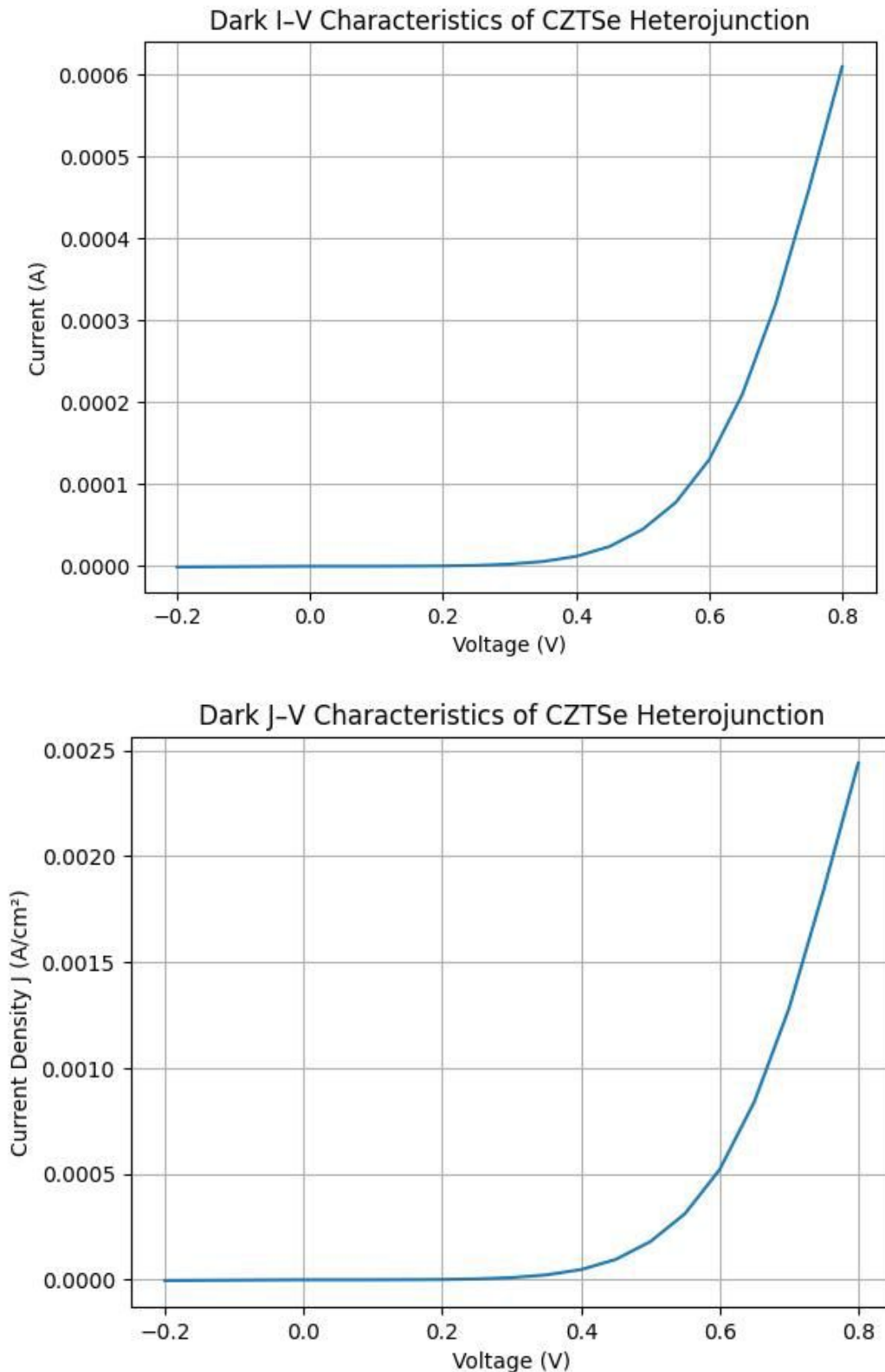


Figure 4. Dark current–voltage (I–V) and current density–voltage (J–V) characteristics of the $\text{Cu}_2\text{ZnSnSe}_4$ heterojunction, demonstrating nonlinear diode-like behavior under forward bias and low leakage current in reverse bias.

3.2 Semi-logarithmic and $\ln(I)$ –V Analysis

The semi-logarithmic representation of the I–V characteristics (Figure 4) reveals a quasi-linear region over a specific voltage range. This behavior indicates exponential carrier transport governed by thermally activated processes. The linear region confirms

that the dominant conduction mechanism in this voltage range follows typical diode-like behavior associated with semiconductor heterojunctions [9,10].

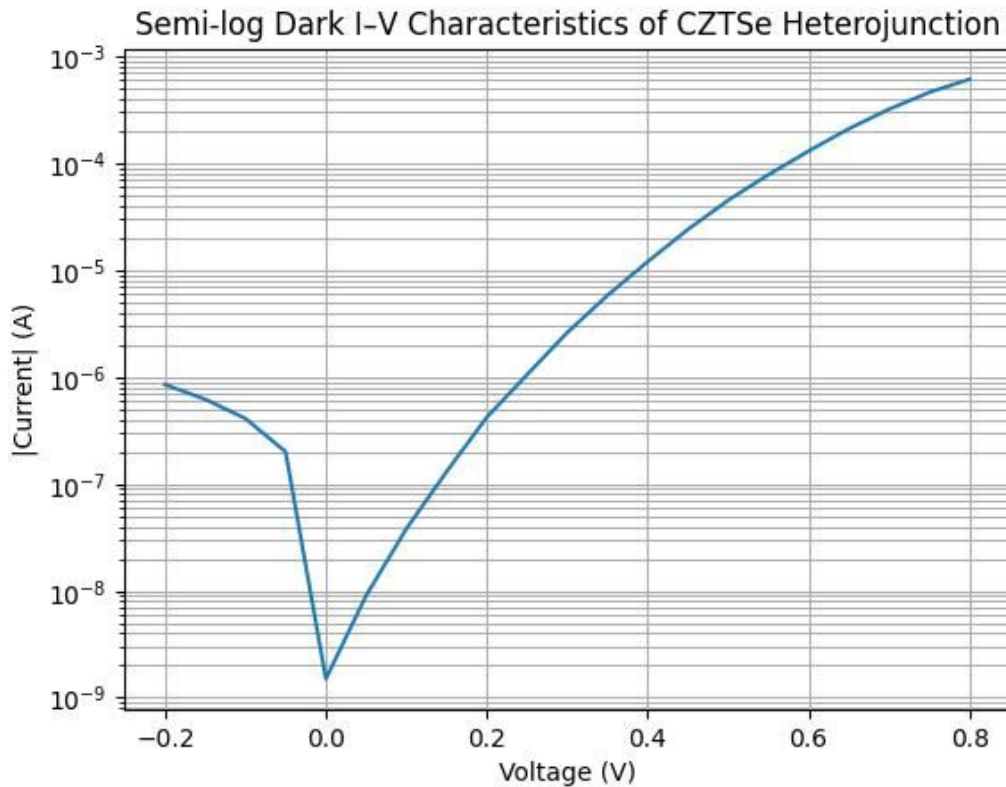


Figure 5. Semi-logarithmic representation of the dark I–V characteristics of the Cu₂ZnSnSe₄ heterojunction showing a linear region corresponding to exponential carrier transport.

3.3 ln(I)–V Analysis and Electrical Parameter Extraction

To obtain quantitative insight into the carrier transport mechanisms, the diode parameters were extracted from the dark I–V characteristics based on the thermionic emission model[6,8,11]:

$$I = I_0 \exp\left(\frac{qV}{nkT}\right)$$

Figure 6. ln(I)–V dependence of the Cu₂ZnSnSe₄ heterojunction under forward bias indicating a linear region used for extraction of diode parameters. From the linear region of the ln(I)–V dependence, the slope was determined:

$$slope = \left(\frac{\ln(I)}{V}\right)$$

Using representative points from the linear region:

$$\begin{aligned} \Delta \ln(I) &\approx 6.5 \\ \Delta V &\approx 0.4 \text{ V} \end{aligned}$$

$$slope \approx \left(\frac{6.5}{0.4}\right) \approx 16.25$$

The ideality factor was calculated using the standard thermionic emission relation

$$n = \frac{\left(\frac{q}{kT}\right)}{slope}$$

At room temperature (T ≈ 300 K):

$$\frac{q}{kT} \approx 38.7$$

Therefore:

$$n \approx \left(\frac{38.7}{16.25} \right) \approx 2.38 \approx 2.4$$

The obtained ideality factor indicates non-ideal diode behavior governed predominantly by recombination processes and interface-related transport mechanisms [12,13], which are commonly observed in kesterite-based heterojunction structures

The saturation current was extracted from the intercept of the $\ln(I)$ - V plot:

$$\begin{aligned} \ln(I_0) &\approx -16 \\ I_0 &\approx \exp(-16) \approx 1 \times 10^{-7} \text{ A} \end{aligned}$$

The effective barrier height was estimated using the thermionic emission framework [6,8]:

$$I_0 = AA^*T^2 \exp\left(\frac{-q\Phi_b}{kT}\right)$$

Rearranging:

$$\Phi_b = \left(\frac{kT}{q}\right) \ln\left(\frac{AA^*T^2}{I_0}\right)$$

The effective barrier height was estimated within the thermionic emission framework.

$$\Phi_b \approx 0.8 \text{ eV}$$

This value confirms the formation of a stable potential barrier at the heterointerface, consistent with thermally activated carrier transport mechanisms.

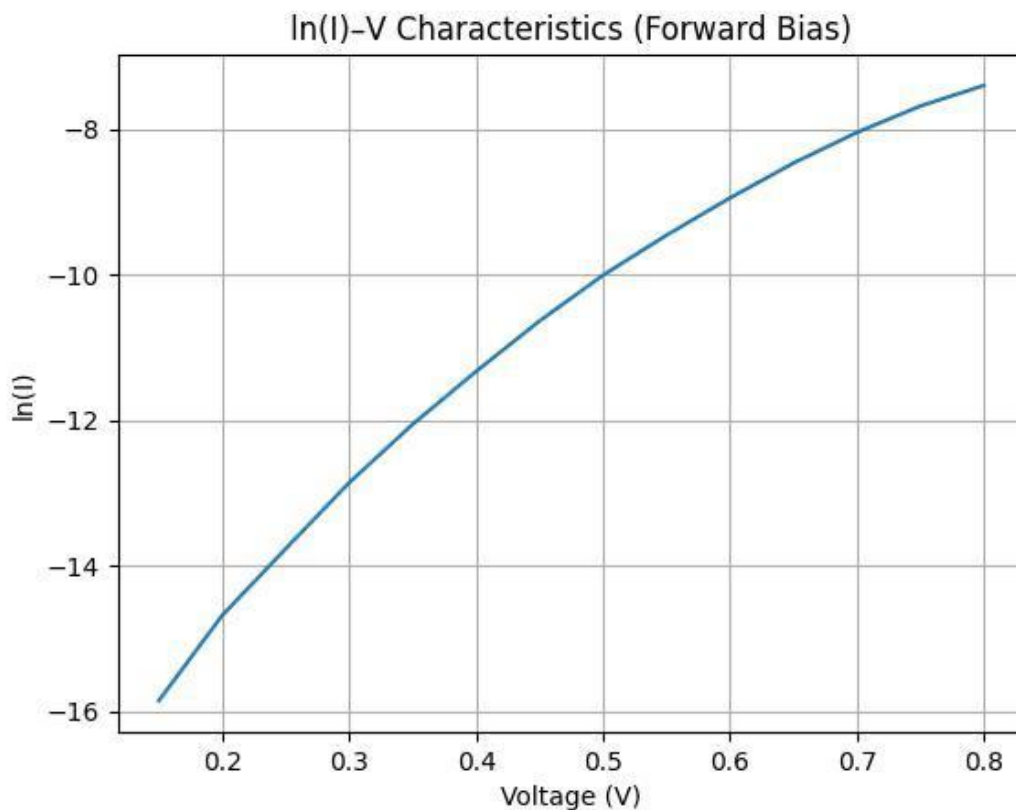


Figure 6. $\ln(I)$ - V dependence of the $\text{Cu}_2\text{ZnSnSe}_4$ heterojunction under forward bias indicating a linear region used for extraction of diode parameters.

3.4 Series Resistance Analysis

At higher forward bias voltages, noticeable deviations from ideal exponential behavior are observed in the I–V characteristics, indicating the increasing influence of series resistance (R_s). These deviations arise due to resistive components associated with the bulk absorber layer, electrical contacts, and interface regions. The series resistance was quantitatively evaluated from the high-bias region of the differential resistance (dV/dI) characteristics [14,15], where the contribution of R_s becomes dominant. The extracted value was found to be:

$$R_s \approx 60 \Omega$$

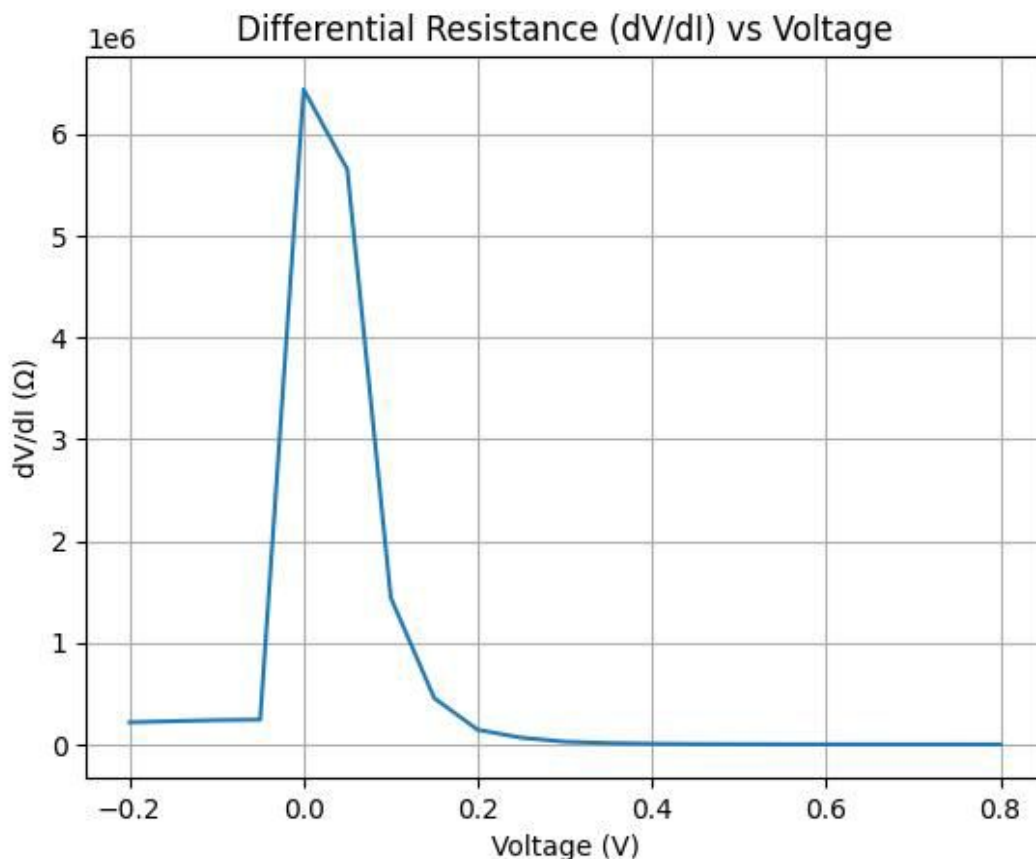
The presence of series resistance leads to a reduction in the effective voltage across the junction, thereby limiting the current flow at higher bias levels. This effect contributes to the observed deviation from ideal diode behavior and plays a significant role in determining the overall electrical performance of the heterojunction.

Furthermore, the influence of R_s is particularly important for device operation under practical conditions, as it directly affects power dissipation and transport efficiency. Therefore, minimizing series resistance through improved contact engineering and interface optimization is essential for enhancing device performance.

3.5 Differential Transport Analysis

Differential conductance (dI/dV) and differential resistance (dV/dI) characteristics are shown in Figure 7. The differential conductance increases with applied voltage, indicating progressive activation of carrier transport due to barrier reduction. Conversely, the differential resistance decreases with increasing voltage, reflecting improved conductivity of the heterojunction. These results confirm that carrier transport is governed by voltage-dependent mechanisms [16,17,24,25] and strongly influenced by interface-controlled processes.

Importantly, differential analysis provides enhanced sensitivity to non-ideal transport behavior that is not fully captured by conventional I–V analysis.



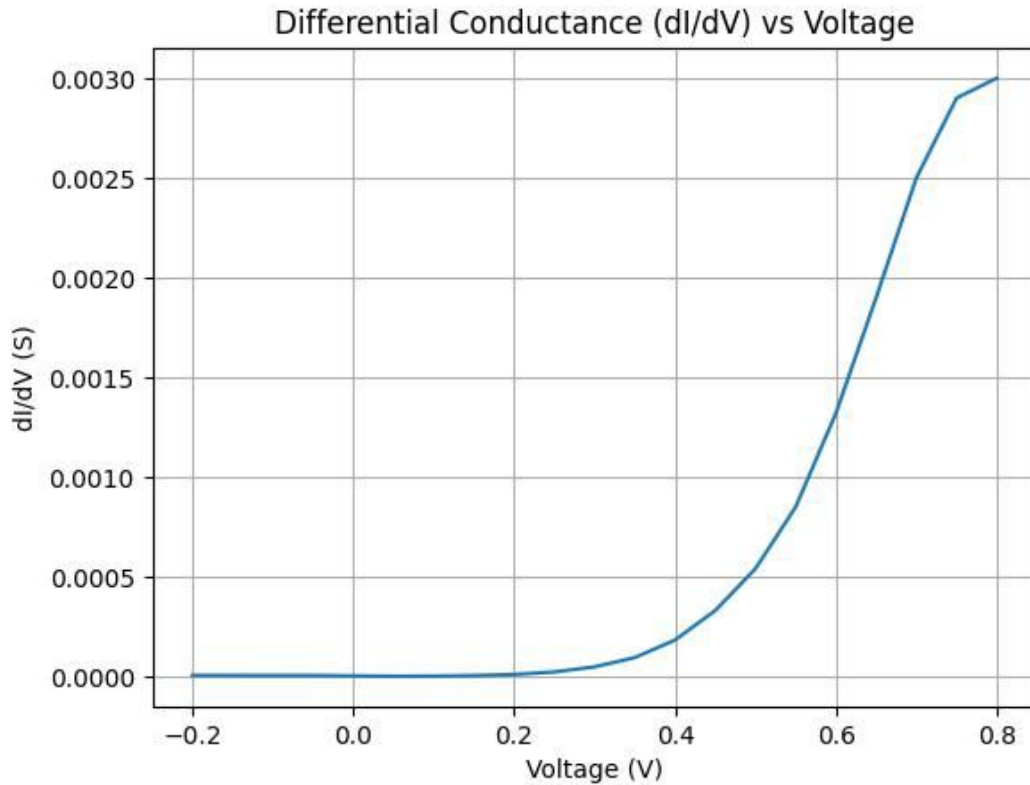


Figure 7. Differential conductance (dI/dV) and differential resistance (dV/dI) as a function of applied voltage for the $Cu_2ZnSnSe_4$ heterojunction.

3.6 Photovoltaic Response under AM1.5G Illumination

The J–V characteristics under AM1.5G illumination are shown in Figure 8. Under illumination, the heterojunction exhibits a clear photovoltaic response, characterized by the generation of photocurrent and the appearance of open-circuit voltage. This behavior confirms effective photogeneration and separation [5,6] of charge carriers. The comparison between dark and illuminated characteristics demonstrates the presence of an additional photo-generated current component, while maintaining diode-like transport behavior.

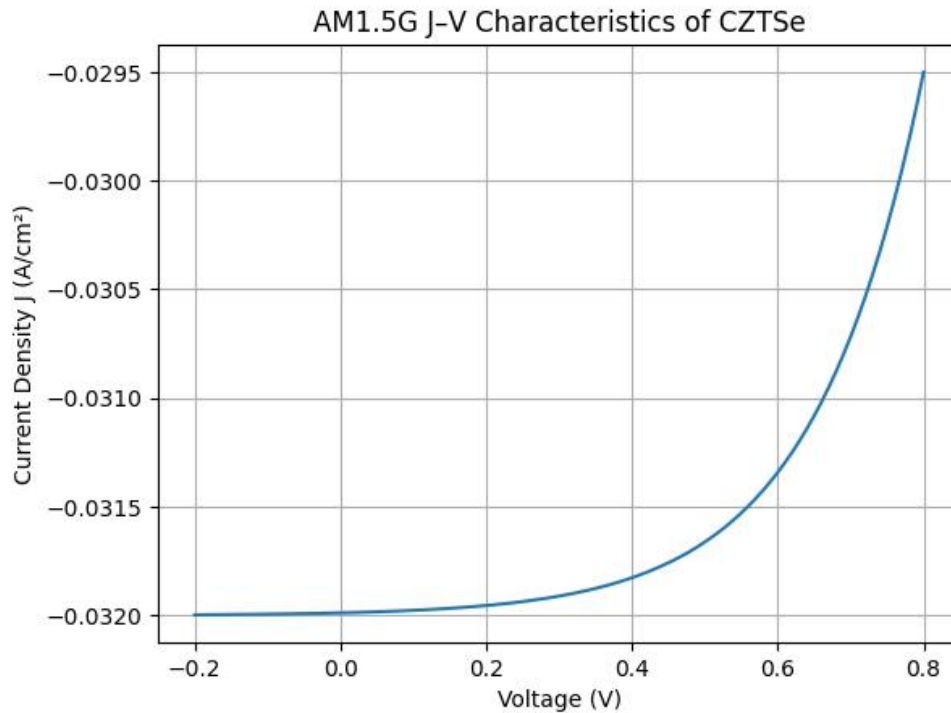


Figure 8. Current density–voltage (J–V) characteristics of the $\text{Cu}_2\text{ZnSnSe}_4$ heterojunction under AM1.5G illumination showing photovoltaic response.

3.7 Physical Interpretation of Transport Mechanisms

The electrical transport behavior of the $\text{Cu}_2\text{ZnSnSe}_4$ (CZTSe)-based heterojunction reflects the combined influence of interface-related recombination, barrier-controlled conduction, and resistive effects. The extracted ideality factor ($n \approx 2.4$) indicates a deviation from ideal diode behavior, pointing to dominant recombination activity within the space-charge region and at the heterointerface [12,13]. This suggests that carrier transport is not solely governed by pure thermionic emission, but is significantly affected by defect-assisted processes. Such behavior is consistent with the presence of localized states introduced by structural disorder and interface imperfections, which facilitate carrier trapping and recombination, thereby limiting transport efficiency.

In addition, the observed transport characteristics at higher bias voltages indicate a growing contribution of resistive effects, which reduce the effective electric field across the junction and modify the current transport regime. The analysis of differential parameters further supports the presence of voltage-dependent conduction [16,17,24], indicating that the transport process evolves with applied bias due to progressive modification of the potential barrier.

Overall, the results highlight that the dominant limitations in the CZTSe heterojunction arise from interface-controlled processes and defect-related recombination pathways [12,13,15]. Therefore, controlling interface quality and reducing defect density are key factors for improving charge transport and overall device performance.

4. CONCLUSION

The electrical transport and photovoltaic behavior of the $\text{Cu}_2\text{ZnSnSe}_4$ (CZTSe)-based heterojunction were systematically investigated using dark I–V characterization, semi-logarithmic analysis, and differential transport techniques. The results demonstrate clear diode-like behavior, confirming the formation of a well-defined potential barrier at the heterointerface.

The extracted ideality factor ($n \approx 2.4$) indicates pronounced non-ideal transport dominated by recombination processes and interface-related defect states. The saturation current ($I_0 \approx 1 \times 10^{-7}$ A) and barrier height ($\Phi_b \approx 0.8$ eV) further confirm thermally activated carrier transport governed by barrier-controlled conduction.

At higher forward bias, deviations from ideal exponential behavior are attributed to series resistance effects ($R_s \approx 60 \Omega$), reflecting the influence of bulk resistance, contact limitations, and interface inhomogeneities. Differential conductance and resistance analyses provide enhanced sensitivity to voltage-dependent transport, revealing the strong contribution of interface-controlled mechanisms.

Under AM1.5G illumination, the heterojunction exhibits a clear photovoltaic response, characterized by effective photogeneration and separation of charge carriers.

Overall, the performance of the CZTSe heterojunction is primarily limited by interface recombination, defect-assisted transport, and resistive losses. Therefore, improving interface quality, reducing defect density, and minimizing series resistance are essential for enhancing device efficiency. These findings provide important physical insight into non-ideal transport mechanisms and support the development of high-performance kesterite-based thin-film solar cells.

ABBREVIATIONS

The following abbreviations are used in this manuscript:

- I–V — Current–voltage
- J–V — Current density–voltage
- CZTSe — $\text{Cu}_2\text{ZnSnSe}_4$
- CZTSSe — $\text{Cu}_2\text{ZnSn}(\text{S},\text{Se})_4$
- DC — Direct current
- dI/dV — Differential conductance
- dV/dI — Differential resistance
- AM1.5G — Air mass 1.5 global solar spectrum
- R_s — Series resistance
- I_0 — Saturation current
- Φ_b — Barrier height
- n — Ideality factor
- q — Elementary charge
- k — Boltzmann constant
- T — Absolute temperature

Conflict of Interest: The authors declare that they have no conflict of interest.

REFERENCES

- [1] S. Chander, et al., *Mater. Today Sustainability*, 2024.
- [2] S. Chander, et al., *Adv. Mater. Interfaces*, 2023.
- [3] Z. Wang, et al., *Nano Energy* 94, 106898 (2022).
- [4] K. Yin, et al., *J. Mater. Chem. A* 10, 779 (2022).
- [5] S. Campbell, et al., *ACS Appl. Energy Mater.* 5, 5404 (2022).
- [6] M. Oubakalla, et al., *Optik* 258, 168886 (2022).
- [7] A. El-Denglawey, et al., *ECS J. Solid State Sci. Technol.* 11, 44006 (2022).
- [8] M. He, et al., *Adv. Sci.* 8, 2004313 (2021).
- [9] A. A. Akl, et al., *Optik* 227, 165837 (2021).
- [10] F. Liu, et al., *Sci. Bull.* (2020).
- [11] O. K. Simya, et al., *Mater. Res. Express* (2020).
- [12] A. V. Stanchik, et al., *Sol. Energy* (2020).
- [13] H. J. Jeong, et al., *Micromachines* (2020).
- [14] I. M. El Radaf, *J. Mater. Sci. Mater. Electron.* 31, 3228 (2020).
- [15] X. Liu, et al., *Prog. Photovolt. Res. Appl.* 24, 879 (2016).
- [16] S. Siebentritt, *Thin Solid Films* 535, 1 (2013).
- [17] S. Levchenko, et al., *Opt. Mater.* 40, 76 (2015).
- [18] S. Sahayaraj, et al., *Sol. Energy Mater. Sol. Cells* 171, 136 (2017).
- [19] B. Saha, et al., *Appl. Surf. Sci.* 418, 328 (2017).
- [20] L. Grenet, et al., *ACS Appl. Energy Mater.* 1, 2103 (2018).
- [21] S. K. Lee, et al., *Sol. Energy Mater. Sol. Cells* (2018).
- [22] A. Ashery, et al., *Silicon* 11, 2567 (2018).
- [23] H. I. Elsaedy, *J. Mater. Sci. Mater. Electron.* 30, 12545 (2019).
- [24] I. M. El Radaf, et al., *J. Electron. Mater.* 48, 6480 (2019).
- [25] I. T. Zedan, et al., *Opto-Electron. Rev.* 27, 348 (2019).